Acta Biomaterialia 127 (2021) 169–179

Contents lists available at ScienceDirect

Acta Biomaterialia

journal homepage: www.elsevier.com/locate/actbio

Full length article

Combined blockade of complement C5 and TLR co-receptor CD14 synergistically inhibits pig-to-human corneal xenograft induced innate inflammatory responses

Rakibul Islam[a,*], Mohammad Mirazul Islam[b,c,d], Per H. Nilsson[a,e,f], Camilla Mohlin[e,f], Kjersti Thorvaldsen Hagen[g], Eleftherios I. Paschalis[c,d], Russell L. Woods[c,d], Sabuj Chandra Bhowmick[h], Claes H. Dohlman[b,d], Terje Espevik[i], James Chodosh[b,d], Miguel Gonzalez-Andrades[b,c,d,j,1], Tom Eirik Mollnes[a,i,k,l,1]

[a] Department of Immunology, Oslo University Hospital and University of Oslo, Oslo, Norway
[b] Massachusetts Eye and Ear, Boston, MA, United States
[c] Schepens Eye Research Institute, Boston, MA, United States
[d] Department of Ophthalmology, Harvard Medical School, Boston, MA, United States
[e] Linnaeus Centre for Biomaterials Chemistry, Linnaeus University, Kalmar, Sweden
[f] Department of Chemistry and Biomedicine, Linnaeus University, Kalmar, Sweden
[g] Department of Pathology, Oslo University Hospital/University of Oslo, Oslo, Norway
[h] Department of Mathematics, University of Oslo, Oslo, Norway
[i] Centre of Molecular Inflammation Research, and Department of Clinical and Molecular Medicine, Norwegian University of Science and Technology, Trondheim, Norway
[j] Maimonides Biomedical Research Institute of Cordoba (IMIBIC), Department of Ophthalmology, Reina Sofia University Hospital and University of Cordoba, Cordoba, Spain
[k] Research Laboratory, Nordland Hospital, Bodo, Norway
[l] Faculty of Health Sciences, K. G. Jebsen Thrombosis Research and Expertise Center, University of Tromsø, Tromso, Norway

ARTICLE INFO

Article history:
Received 3 December 2020
Revised 18 February 2021
Accepted 19 March 2021
Available online 27 March 2021

Keywords:
Xenotransplantation
Cornea
Decellularization
Complement system
Toll-like receptor
Cytokine
Regenerative medicine
Biomaterial

ABSTRACT

Inadequate supplies of donor corneas have evoked an escalating interest in corneal xenotransplantation. However, innate immune responses contribute significantly to the mechanism of xenograft rejection. We hypothesized that complement component C5 and TLR co-receptor CD14 inhibition would inhibit porcine cornea induced innate immune responses. Therefore, we measured cytokine release in human blood, induced by three forms of corneal xenografts with or without inhibitors. Native porcine cornea (NPC) induced interleukins (IL-1β, IL-2, IL-6, IL-8, IL-1ra), chemokines (MCP-1, MIP-1α, MIP-1β) and other cytokines (TNF, G-CSF, INF-γ, FGF-basic). Decellularized (DPC) and gamma-irradiated cornea (g-DPC) elevated the release of those cytokines. C5-blockade by eculizumab inhibited all the cytokines except G-CSF when induced by NPC. However, C5-blockade failed to reduce DPC and g-DPC induced cytokines. Blockade of CD14 inhibited DPC-induced cytokines except for IL-8, MCP-1, MIP-1α, and G-CSF, while it inhibited all of them when induced by g-DPC. Combined blockade of C5 and CD14 inhibited the maximum number of cytokines regardless of the xenograft type. Finally, by using the TLR4 specific inhibitor Eritoran, we showed that TLR4 activation was the basis for the CD14 effect. Thus, blockade of C5, when combined with TLR4 inhibition, may have therapeutic potential in pig-to-human corneal xenotransplantation.

Statement of significance

Bio-engineered corneal xenografts are on the verge of becoming a viable alternative to allogenic human-donor-cornea, but the host's innate immune response is still a critical barrier for graft acceptance. By

* Corresponding author at: Complement Research Group, Department of Immunology, Oslo University Hospital (Rikshospitalet), Sognsvannsveien 20, 0372 Oslo, Norway.
E-mail address: rakibul.lubikar@gmail.com (R. Islam).
[1] These authors contributed equally to the manuscript.

https://doi.org/10.1016/j.actbio.2021.03.047

overruling this barrier, limited graft availability would no longer be an issue for treating corneal diseases. We showed that the xenograft induced inflammation is initiated by the complement system and toll-like receptor activation. Intriguingly, the inflammatory response was efficiently blocked by simultaneously targeting bottleneck molecules in the complement system (C5) and the TLR co-receptor CD14 with pharmaceutical inhibitors. We postulate that a combination of C5 and CD14 inhibition could have a great therapeutic potential to overcome the immunologic barrier in pig-to-human corneal xenotransplantation.

1. Introduction

Corneal diseases stand as one of the leading causes of blindness worldwide. Still today, the gold-standard treatment for corneal blindness is transplantation [1]. However, because of a lack of donors, 12.7 million people await treatment to restore their vision [2]. In this context, corneal xenograft emerges as an accessible alternative to human allografts. In the early period of corneal xenotransplantation, several alternatives of human-donor-cornea from various non-human species were tested for feasibility, but without success in restoring vision [3–8]. However, recent progress in bioengineering and immunology has led to a renewed interest in corneal xenotransplantation with promising results in pre-clinical and clinical studies [9–13]. Hence, a better understanding of the recipient's immune reaction towards the corneal xenograft is crucial.

In this regard, decellularization enables complete or partial removal of cellular and immunogenic components from the corneal xenograft while preserving extracellular matrix with its native micro- and macroscopic structure [14–16]. The decellularized cornea can serve as an *in vivo* scaffold for tissue regeneration that maintains the physiological properties required to replace the target organ [17]. In order to bring decellularized corneas into the clinic, an additional step of sterilization is necessary to reduce the risk of graft-associated infections in human recipients. Gamma irradiation, a well-standardized sterilization method, had been applied to decellularized xenografts implanted into human patients [13]. Though it is not a routine procedure in human donor corneal transplantation, patients that received gamma-irradiated human cornea showed favourable outcomes without graft rejection, loss of transparency, or neovascularization [18], and with reduced allogenicity [19].

Data from pre-clinical studies suggest that the complement system, a backbone of innate immunity, might play a role in corneal xenograft rejection [14,20,21]. The complement system is functional in the aqueous humor of the eye [22], but corneal tissue protects against self-attack by membrane-bound complement regulatory proteins (CD46, CD55, and CD59) [23,24]. If a corneal xenograft is placed onto a high risk-patient, usually with a neovascularized and inflamed host bed, the plasma complement system will gain immediate access to the graft with a possible subsequent risk of activation. Another integral part of the innate immune system is the toll-like receptor (TLR) system, which has not been thoroughly investigated in the corneal xenotransplantation context. Also, an association of increasing levels of extracellular histones with xenotransplantation is known, and this may elevate systemic inflammation by histone-dependent activation of TLR2, 4, and 9 [25,26].

Thus, there is a critical need for understanding the human innate immune response to corneal xenograft in order to avoid graft rejection, and to facilitate its success in human patients. The acute innate immune responses towards porcine cornea can be evaluated by incubation in fresh human whole blood. In this study, we assessed the human acute inflammatory response, including the innate immune response, toward three forms of porcine corneal xenograft, in whole blood *ex vivo* with a focus on complement and TLR-mediated pathways. Porcine xenograft was chosen because it is the most widely used in pre-clinical and clinical research based on its similarities to human cornea [27]. Despite regularly using decellularization and irradiation techniques for the manufacturing of xenografts, we wanted to understand the implications of the different steps in this process and create controls to follow the modifications in the different variables that we evaluated.

2. Materials and methods

2.1. Preparation of corneas

Fresh porcine eyes were collected immediately after the death of the pigs at the slaughterhouse. The eyes were kept in phosphate buffer saline (PBS) inside a box of wet ice until the decellularization process was performed, as detailed elsewhere [15]. Briefly, selected corneas were removed from pig eyes with a 16 mm diameter trephine and washed with PBS. From each 16 mm piece of the cornea, three 6 mm diameter pieces were cut; among them, one piece was used as a native porcine cornea (NPC), preserved in glycerol without further processing. The remaining two pieces underwent the decellularization process. Each cornea piece was placed in a well of a 12-well plate, facing epithelial side down. Sodium Dodecyl Sulphate (SDS) 0.1% (Applied Biosystems, CA) in dH_2O was added to the wells. After 72 h, SDS was replaced by PBS and maintained for 48 h. The solution was 2 ml in volume and changed every 24 h. During the process of decellularization, the plate containing the pieces of cornea were kept under continuous shaking (60 rpm) on Orbit LS (Labnet International Inc., NJ) at room temperature. After the completion of the process, the decellularized porcine cornea (DPC) was immersed into 100% glycerol in 1.5 ml Eppendorf tubes for dehydration and kept at room temperature without shaking until further processing.

One of the DPCs was sterilized by gamma irradiation using a Cobalt-60 source (MDS Nordion Gammacell 220E irradiator at the Massachusetts Institute of Technology, Department of Biological Engineering; Cambridge, MA) at room temperature (g-DPC). The dose was calculated according to the cobalt-60 source decay calculation, and 25 kGy was chosen for the sterilization of DPC [15].

2.2. Morphological analysis of the corneas

Transmission electron microscopy was performed on random samples of NPC, DPC, and g-DPC. All cornea samples were fixed with half-strength Karnovsky's fixative (2% formaldehyde + 2.5% glutaraldehyde, in 0.1 M sodium cacodylate buffer, pH 7.4; Electron Microscopy Sciences, Hatfield, PA) at room temperature for 30 min, and then placed in fresh Karnovsky's fixative for 4 h. The samples were washed thrice with 0.1 M cacodylate buffer for 5 min at room temperature. After additional washing with PBS, specimens were post-fixed with 2% osmium tetroxide in 0.1 M sodium cacodylate buffer for 1.5 h at room temperature, *en bloc* stained with 2% aqueous uranyl acetate for 30 min, then dehydrated with

graded ethyl alcohol solutions, and embedded in tEPON-812 epoxy resin (Tousimis, Rockville, MD) using an automated EMS Lynx 2 EM tissue processor (Electron Microscopy Sciences). Ultrathin sections (80 nm) were cut from each sample block using a Leica EM UC7 ultramicrotome (Leica Microsystems, Buffalo Grove, IL) and a diamond knife and mounted on copper grids and air-dried. The thin sections on grids were stained with aqueous 2.5% aqueous gadolinium acetate hydrate and Sato's lead citrate stains using a modified Hiraoka grid staining system [28]. Sections were observed by an FEI Tecnai G2 Spirit transmission electron microscope (FEI, Hillsboro, OR) at 80 kV interfaced with an AMT XR41 digital CCD camera (Advanced Microscopy Techniques, Woburn, MA) for digital TIFF file image acquisition.

2.3. Incubation of corneas in whole blood, plasma preparation, and histological evaluation

The study was performed with the consent (S-04114) of the regional ethical committee, South-Eastern Norway Regional Health Authority. Human blood was drawn from healthy donors into polypropylene tubes (Nunc™, Thermofisher, MA) containing a specific thrombin inhibitor, lepirudin (Refludan®, Celgene, Uxbridge, U.K.) at a final concentration of 50 µg/mL [29]. For each set of experiments, 300 µL of the blood was aliquoted into individual 1.8-mL round-bottom sterile polypropylene cryogenic tubes (Nunc® Cryotubes®, Merck, Darmstadt, Germany) and incubated at 37 °C with either NPC, DPC, or g-DPC. The cornea incubations were performed with or without eculizumab at 100 µg/mL (Soliris®, Alexion Pharma GmbH, Zürich, Switzerland) and anti-CD14 antibodies (r18D11 at 15 µg/mL) [30]. A common IgG2/4 isotype control, (NHDL) on the similar IgG2/4-structure as eculizumab and r18D11, was used as control for both antibodies [31]. Eritoran (a kind gift from Eisai Co. Tokyo, Japan), an antagonist for TLR4, was used at 1.3 µg/mL concentration to compare the effect with CD14 inhibition [32].

Blood was sampled either at 30 min or after one-hour incubation for complement activation analysis, and the corneas were further incubated until four hours for cytokine analysis. Two sets of negative controls were used, one without treatment: fresh blood used to measure the initial complement activation before starting the incubation; and the background activation: the activation in the blood during the same incubation time under the same conditions but without corneas. Zymosan and lipopolysaccharide (LPS) at 100 µg/mL and 150 ng/mL concentration, served as positive controls for complement activation and cytokine release, respectively. After incubation, ethylenediaminetetraacetic acid (EDTA) at 10 mM final concentration was added to the blood at the end of each incubation to stop further complement activation. Sampled blood was centrifuged at 3000 x *g* at 4 °C to separate the plasma, which was collected in individual tubes and preserved at −70 °C until further analysis.

Corneas were histologically evaluated before and after incubation with whole blood. The corneas were embedded in cryopreserving solution (OCT medium, VWR, Oslo, Norway) after thoroughly washing with PBS. They were sectioned at 10 µm using a microtome and then placed on glass cover slides. Hematoxylin (VWR international, Leuven, Belgium), azophloxin (Sigma-Aldrich, St. Louis, MO), and Saffron (Waldeck, Münster, Germany) commonly referred as HAS staining were used for staining cell nuclei, soft tissue, and connective tissue, respectively [33].

2.4. Complement activation

Complement activation was detected both on the surface of the cornea and in the fluid phase in plasma collected after whole blood incubation. Fresh frozen corneas were embedded in cryomount™ (HistoLab, Gothenburg, Sweden) cryosectioned at 10 µm, allowed to dry, and stored at −80 °C. Primary antibodies for C3d 1:1000 (Dako, Glostrup, Denmark), C4d 1:1000 (Spring Biosciences Corp, Suit Pleasanton, CA) and mAb aE11 (reacting with a neoepitope exposed in C9 when incorporated into the terminal C5b-9 complement complex) 1:250 (Diatec Monoclonals AS, Oslo, Norway) were incubated with the specimens overnight at 4 °C. After rinsing in PBS (Sigma-Aldrich), sections were incubated with selected fluorescent-dye conjugated secondary antibodies: Alexa Fluor® 488 conjugated donkey anti-rabbit IgG 1:500 (Invitrogen, Carlsbad, CA), or with Alexa Fluor® 568 conjugated goat anti-mouse IgG Fab 1:500 (Invitrogen) at room temperature for 45 min in the dark. All antibodies were diluted in blocking solution (1% BSA (Sigma) in PBS). Specimens were rinsed in PBS and mounted by using the nuclear staining 4', 6-diamidino-2-phenylindole (DAPI) mounting medium (Vector Laboratories, Burlingame, CA). The omission of the primary antibody served as a negative control in all experiments. Corneal sections were assessed in an epifluorescence microscope (Nikon, Tokyo, Japan) equipped with applicable filters. Images were captured with a digital acquisition system (DS-U1, Optronics) and the software Nis elements 4.30 (Nikon).

In the fluid phase, complement activation at the levels of C4 (generated either via classical or lectin pathway), C3 of the final common pathway, and terminal complement complex of the terminal pathway were analyzed by quantification of C4bc, C3bc, and sC5b-9 respectively, in EDTA-plasma samples using ELISA as described previously [29,34]. Briefly, the assays were based on monoclonal antibodies detecting neo-epitopes exposed after activation, hence, specifically measuring only components formed upon activation. C4bc was immobilized using a mAb (gift from Prof. Dr. C. E. Hack) for a neoepitope exposed on activation products C4b, C4bi, C4c (C4bc) as well as on iC4, but not on native C4 [35]. An addition of a polyclonal biotinylated antibody against C4 was used to identify C4bc. C3bc was determined by sandwich ELISA, using mAb bH6 specific for a neoepitope exposed in C3b, iC3b, and C3c as capture antibody [36], and biotinylated polyclonal anti-C3 and HRP-conjugated streptavidin (GE Healthcare) for detection. Similarly, sC5b-9 was determined using the anti-neo C9 monoclonal antibody aE11 (produced in our laboratory) [37] for capture and biotinylated monoclonal anti C6 (clone 9C4, produced in our laboratory) [38], and finally, the streptavidin-HRP conjugate was added for detection.

2.5. Cytokines induced by the cornea in human whole blood

The EDTA plasma samples were analysed in duplicate using a commercial fluorescence magnetic bead-based immunoassay, with high-sensitivity detection range and precision (Bio-Plex Human Cytokine 27-Plex, Bio-Rad Laboratories Inc., Hercules, CA). The following cytokines were analysed: interleukin (IL)-1 beta (IL-1β), IL-1 receptor antagonist (IL-1ra), IL-2, IL-4, IL-5, IL-6, IL-7, IL-8 (C-X-C motif chemokine ligand 8 CXCL8), IL-9, IL-10, IL-12, IL-13, IL-15, IL-17, eotaxin-1 (C-C motif chemokine ligand 11; CCL11), basic fibroblast growth factor (FGF-basic), granulocyte colony-stimulating factor (GCSF), granulocyte-macrophage colony-stimulating factor (GM-CSF), interferon-gamma (IFN-γ), IFN-γ-inducing protein 10 (IP-10; CXCL10), monocyte chemoattractant protein 1 (MCP-1; CCL2), macrophage inflammatory protein-1-alpha (MIP-1α; CCL3), macrophage inflammatory protein-1-beta (MIP-1β; CCL4), platelet-derived growth factor-BB (PDGF-BB), RANTES (CCL5), tumor necrosis factor (TNF) and vascular endothelial growth factor (VEGF). The analyses were performed according to the manufacturer's instructions.

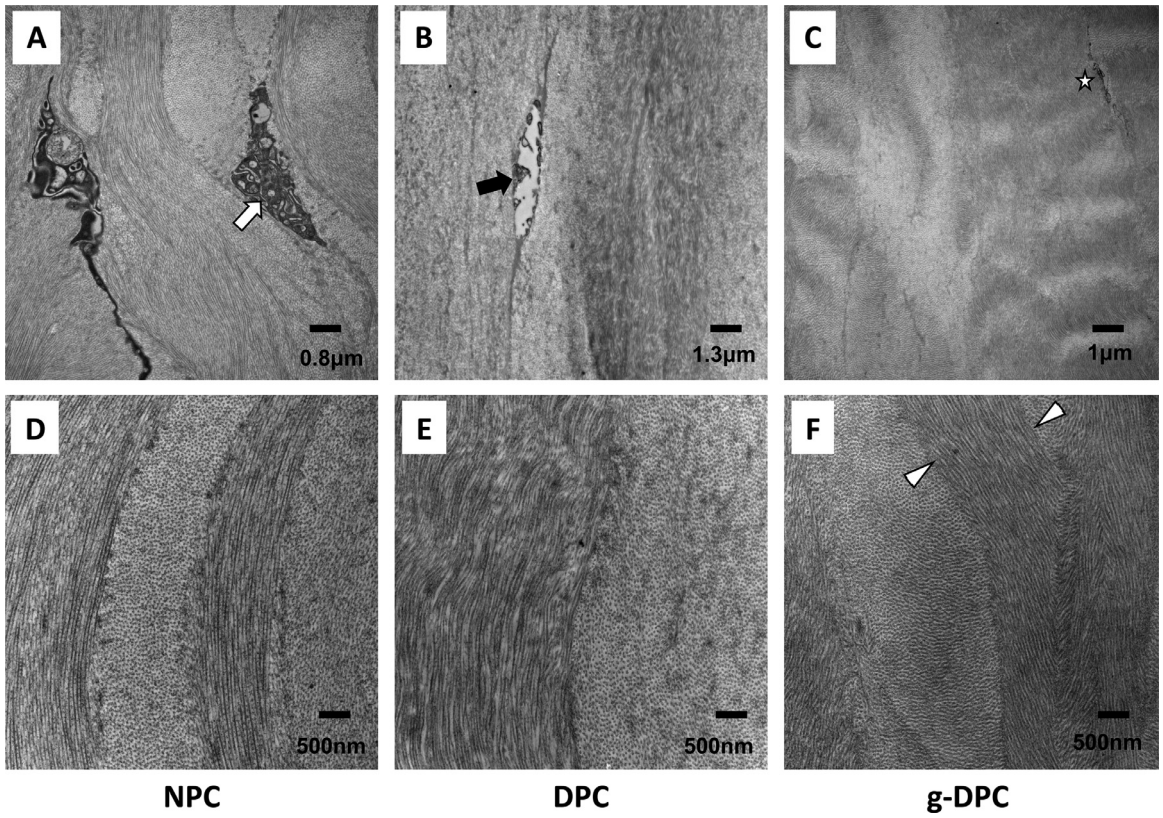

Fig. 1. Transmission electron micrographs of native porcine cornea (NPC), decellularized porcine cornea (DPC), and gamma-irradiated decellularized porcine cornea (g-DPC). Upper panels (A-C) represent low magnification, and lower panels (D-F) represent high magnification. Images of NPC shows a keratocyte -white arrow- (A); presence of debris after decellularization (DPC) -black arrow- (B) and increased space between collagen fibrils after decellularization (E). Gamma irradiation (g-DPC) increased the compactness resulting in disappearance of the empty space created by decellularization, although debris was visualized -white asterisk- (C). Parallel collagen lamellae were observed in NPC (D) and DPC (E) but altered in g-DPC, shown with two white arrowheads (F).

2.6. Limulus amoebocyte lysate assay for detection of LPS

The cornea storing solutions and incubated plasma were tested for LPS by the endpoint chromogenic assay (LAL assay, Lonza, Basel, Switzerland) following the manufacturer's protocol. In each case, the LPS level was below the 0.01 EU /mL, thus below the lower limit of detection. In the 5 µg/mL-LPS-positive control, LPS was detected at 15 EU/mL.

2.7. Statistical analyses

Data were analysed using linear mixed models (mixed-effects linear regression), with human donor as a random effect. In all studies, cornea was confounded with donor in that the blood from each donor was applied to a unique set of corneas. We found that the cytokine concentrations were skewed. Analysis of $\log_{10}$(concentration) led approximately normal distributions and acceptable patterns in the residuals of the models. The linear mixed models produced comparisons between the control condition and all other conditions. Following the linear mixed models, we conducted planned analyses of additional paired comparisons using Wald tests of these simple linear hypotheses. Since there were so many models and planned comparisons ($n = 131$), we adjusted the level for acceptance of significance to $p \leq 0.017$. Our outcome variables were highly correlated, with an average Spearman correlation rho = 0.77 (median 0.82, range 0.36– 0.95). The adjustment was done using the D/AP (Dubey and Armitage-Parmar) method as described by Sankoh, Huque and Dubey [39]. In the figures, we show commonly used significance levels (e.g. 0.05, 0.001) using numbers of stars, as explained in the figure legends, in addition to $p \leq 0.017$.

3. Results

3.1. Morphological analysis

Transmission electron microscopy was used to compare the presence of cells and the fibrillar arrangement of collagen of the stroma of NPC, DPC, and g-DPC (Fig. 1). Keratocytes were apparent in the stroma of NPC (Fig. 1 A), whereas the images of DPC and g-DPC confirmed the removal of keratocytes, leaving vacant spaces inside the stroma (Fig. 1 B and C). Some cellular debris is apparent in the decellularized groups (Fig. 1 B). Overall, organized collagen lamellae were observed in all groups (Fig. 1 D-F). In DPC, the collagen lamellae within the stroma were arranged parallel to each other, similar to the NPC (Fig. 1 D and E). In g-DPC, the parallel nature of the collagen lamellae was partially altered, and compactness between lamellae increased (Fig. 1 F). The collagen interfibrillar distances within the lamellae were increased by decellularization, *i.e.,* DPC compared to NPC but that was counterbalanced by gamma irradiation.

The morphological examination was performed with HAS staining before (Fig. 2A-C) and after (Fig. 2D-F) incubation of corneas in whole blood. NPC showed the epithelial layer stained in red color and keratocytes in the stromal layer in blue (Fig. 2A and D). DPC and g-DPC were free from the cells as expected (Fig. 2B, C, and E, F) with no indication of leukocyte-infiltration after whole blood incubation (Fig. 2D-F).

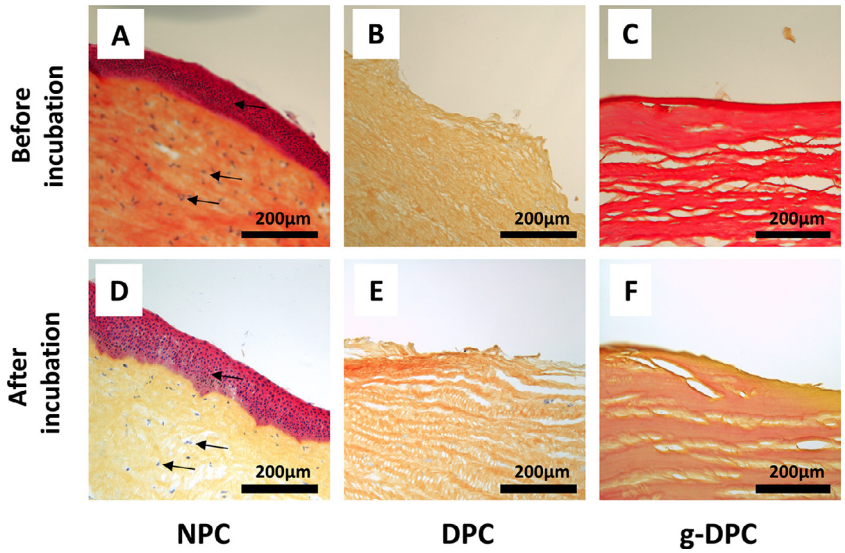

Fig. 2. Bright-field micrographs of the corneas by hematoxylin-azophloxine-saffron (HAS) staining. Upper panels (A-C) show the morphology of native porcine cornea (NPC), decellularized porcine cornea (DPC), and gamma-irradiated decellularized porcine cornea (g-DPC), respectively, before incubation with human whole blood. Lower panels (D-F) show the same corneas after the incubation. Black arrows (A and D) show cells in native corneas (NPC). There was no indication of leukocyte infiltration into the cornea after whole blood incubation (D, E, F). Magnification: x200.

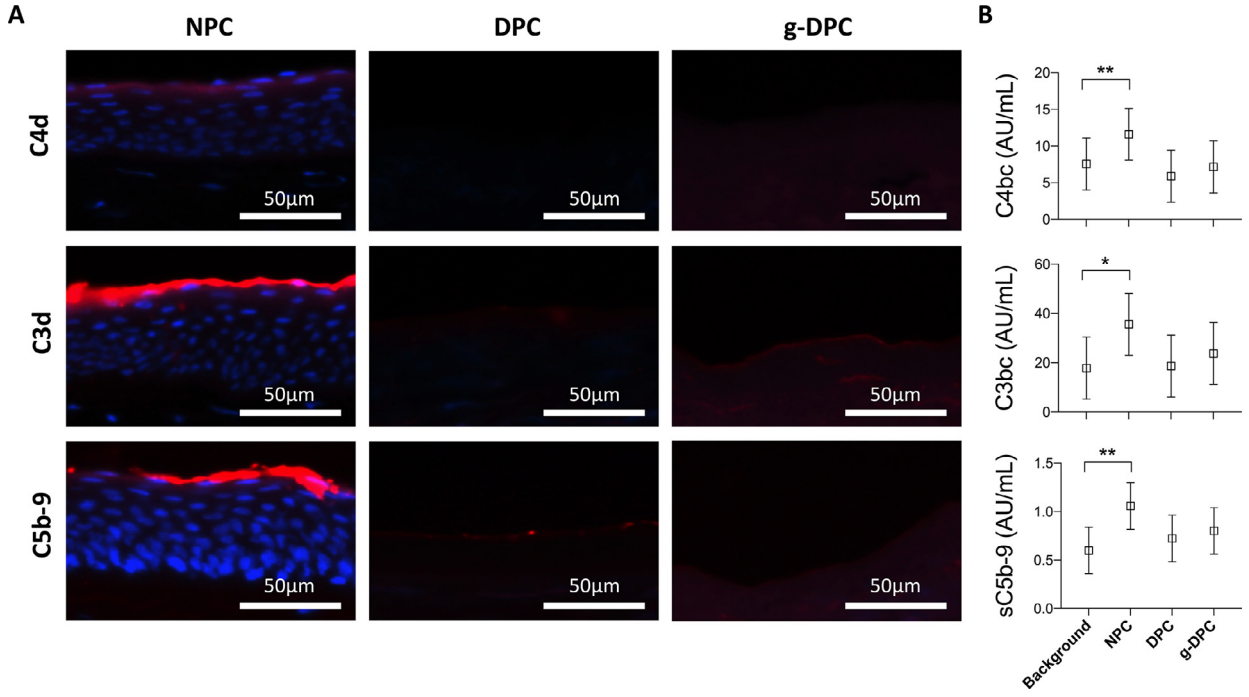

Fig. 3. Complement activation induced by three forms (NPC, DPC, and g-DPC) of porcine cornea in human whole blood. (A) Deposition of the activated fragments of complement proteins C4d, C3d, and C5b-9 on the corneas. Three individual samples of human donor blood were used to evaluate the deposition of the activation fragments on each form of the cornea surface (total of nine porcine cornea pieces). Blue-staining shows the corneal cell nuclei, and red-staining shows the deposited complement-activation fragments on the cornea surface. (B) The level of soluble counterpart for C4-activation (C4bc), C3-activation (C3bc), and terminal pathway activation (sC5b-9) were detected by ELISA. Four individual human donors blood samples were used to evaluate the activation (four corneal samples for each condition). Background activation was the level of activation markers in the blood incubated in the same condition in the absence of the cornea. Data are presented as margin plots. Horizontal lines in boxes represent mean values of each experimental group (background, NPC, DPC, and g-DPC), and the error bars indicate the 95% confidence intervals. Statistical significance was estimated by using the mixed-effect model analysis by comparing the mean of the background activation group with the mean of each other group. Significance levels are denoted as star (*), where * $p \leq 0.05$, ** $p \leq 0.017$. (For interpretation of the references to color in this figure legend, the reader is referred to the web version of this article.)

3.2. Complement activation after incubation of porcine corneas in human whole blood

Deposition of the activated fragments C4d, C3d, and C5b-9 of complement proteins on the corneas and corresponding activated fragments C4bc, C3bc, and sC5b-9 in the fluid phase were detected (Fig. 3). Immunofluorescent staining was seen on the surface of the NPC, C4d being modest, as compared to a strong C3d and C5b-9 deposition (Fig. 3 A). On DPC and g-DPC, complement deposition was hardly detectable (Fig. 3A). The pattern was similar when measured by the fluid phase activation markers: C4bc, C3bc and sC5b-9. C4bc, and sC5b-9 were significantly higher with NPC

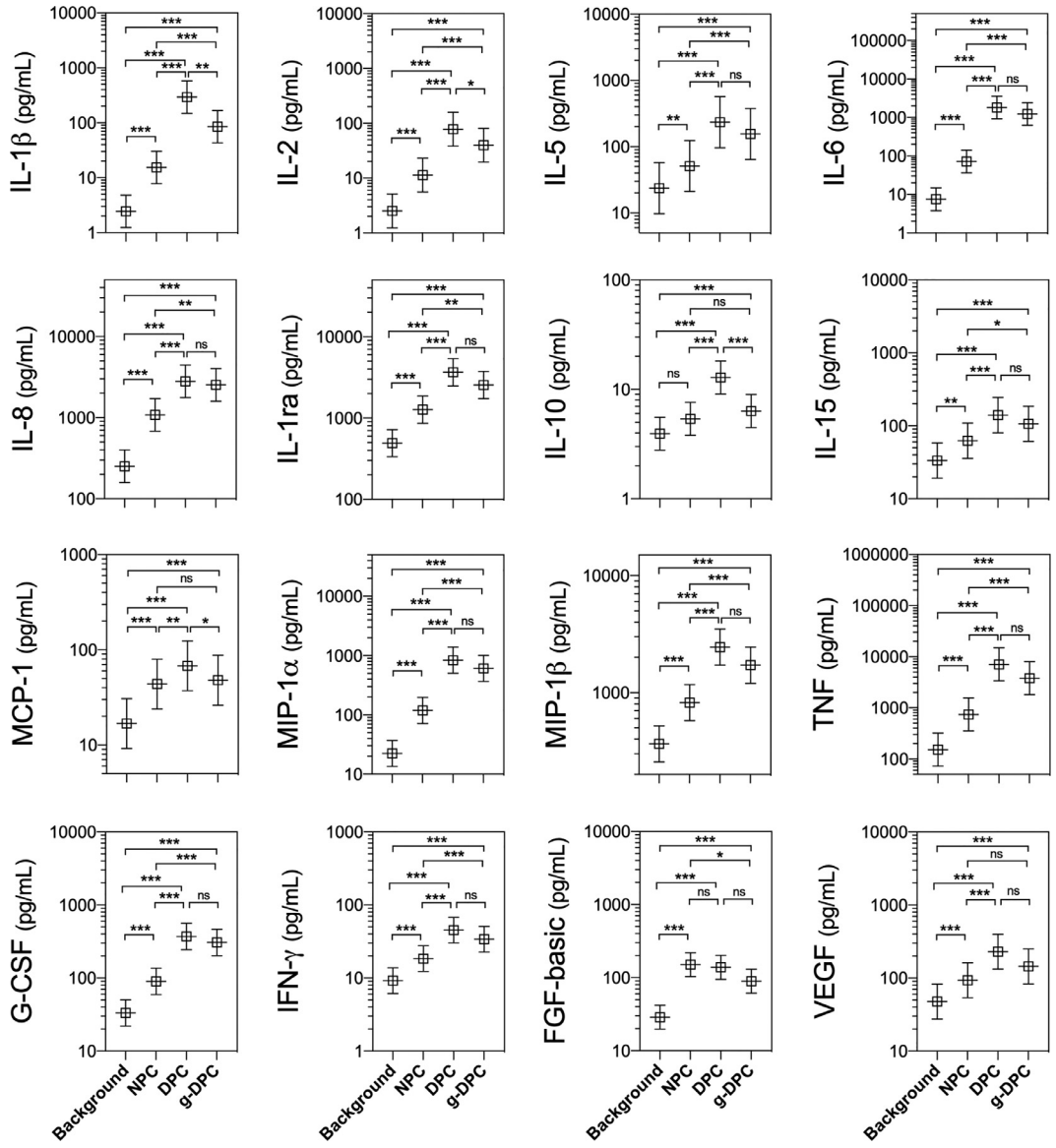

Fig. 4. Cytokine expression induced by three forms (NPC, DPC, and g-DPC) of porcine cornea in human blood. Cytokine levels were detected by using a multiplex assay. Fifteen individual human donor blood samples were used to evaluate cytokine expression by using each form of the cornea (total forty-five porcine cornea pieces). Data are presented as margin plots. Horizontal lines in boxes represent the mean of each experimental condition (background, NPC, DPC, and g-DPC), and the error bars indicate the 95% confidence intervals. Statistical significance was estimated by using mixed-effect models that compared the log-transformed data for the control condition with each other experimental condition, and planned Wald tests of simple linear hypotheses for other paired comparisons. Significance levels are denoted as star (*) where, * $p \leq 0.05$, ** $p \leq 0.017$, and *** $p \leq 0.001$.

($p \leq 0.017$) but not with DPC or g-DPC as compared to incubation of blood in the same condition without cornea, the control condition (Fig. 3 B).

3.3. Cytokine responses after incubation of porcine corneas in human whole blood

We investigated the porcine cornea-induced cytokine release in human whole blood. Of the twenty-seven cytokines examined, sixteen (IL-1β, IL-2, IL-5, IL-6, IL-8, IL-1ra, IL-10, IL-15, MCP-1, MIP-1α, MIP-1β, TNF, G-CSF, IFN-γ, FGF-basic, and VEGF) significantly increased ($p \leq 0.001$) over background levels (incubation of blood in the same condition without cornea) after incubation with decellularized cornea and were selected for further study (Fig. 4). Native porcine cornea also increased the same set of cytokines, except for of IL-10 compared to the background level. All the cytokines, except for FGF-basic, were released at a statistically significantly higher ($p \leq 0.017$) concentration when incubated with DPC compared to the release induced by NPC (Fig. 4).

Interestingly, g-DPC tended to induce a slightly lower level of cytokines compared to DPC; the reduction was statistically significant only for IL-1β and IL-10 ($p \leq 0.017$) but not for rest of the cytokines (Fig. 4). However, among the reduced cytokines, all of them were still significantly higher ($p \leq 0.001$) than the control condition.

3.4. Effect of inhibiting complement, CD14, and TLR4 on the cytokine response

We further tested the effect of inhibition of complement C5 and the TLR system, including CD14 and TLR4 (Figs. 5 and 6). The blockade of C5 and CD14 each inhibited the release of the cytokines induced by NPC. Blockade of C5 alone inhibited ($p \leq 0.017$) fourteen of the sixteen cytokines (IL-1β, IL-2, IL-5, IL-6, IL-8, IL-

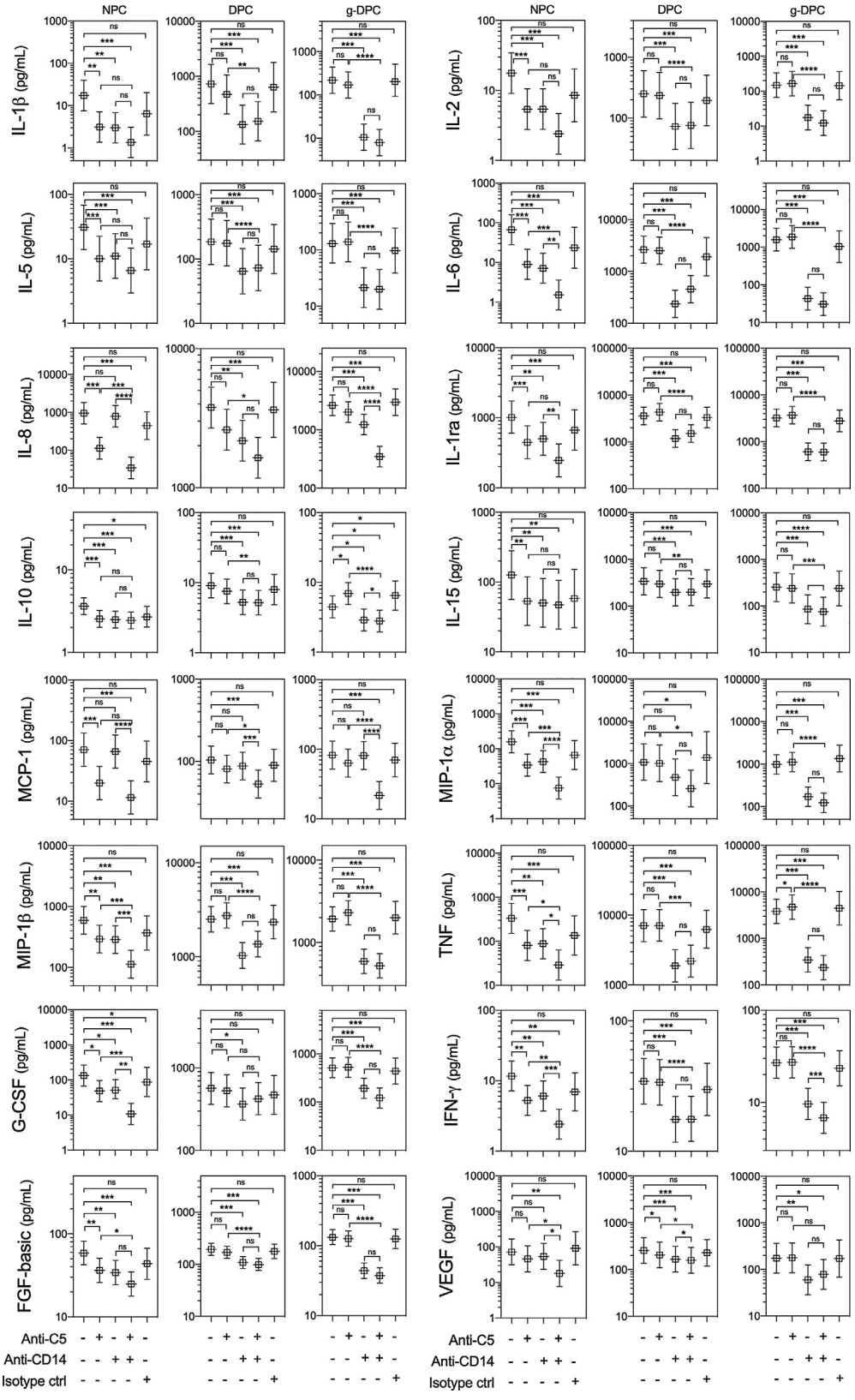

Fig. 5. Effects of C5 and CD14 inhibition alone and in combination on cytokine expression induced by the three forms (NPC, DPC, and g-DPC) of porcine cornea in human whole blood. The level of cytokines was detected by using a multiplex assay. Effects of both inhibitors were measured separately and in combination in eight individual human donor blood samples where cytokine response was induced by each form of cornea (requiring a total of 108 porcine cornea pieces). The effect of isotype controls was evaluated in four individual human donor blood samples. Data are presented as margin plots. Horizontal lines in boxes represent the mean of each form of cornea induced cytokine level without inhibitors (anti-C5–, anti-CD14– and isotype control–), with C5 inhibitor alone (anti-C5+, anti-CD14– and isotype control–), with CD14 inhibitor alone (anti-C5–, anti-CD14+ and isotype control–), with combination of inhibitors (anti-C5+, anti-CD14+ and isotype control–), and with isotype control (anti-C5–, anti-CD14– and isotype control+). The error bars show the 95% confidence intervals. Statistical significance was estimated by using mixed-effect models that compared the log-transformed data for the without-inhibitor condition with every other condition. Significance levels are denoted as star (*) where, $^{*}p \leq 0.05$, $^{**}p \leq 0.017$, $^{***}p \leq 0.001$ and **** $p \leq 0.0001$.

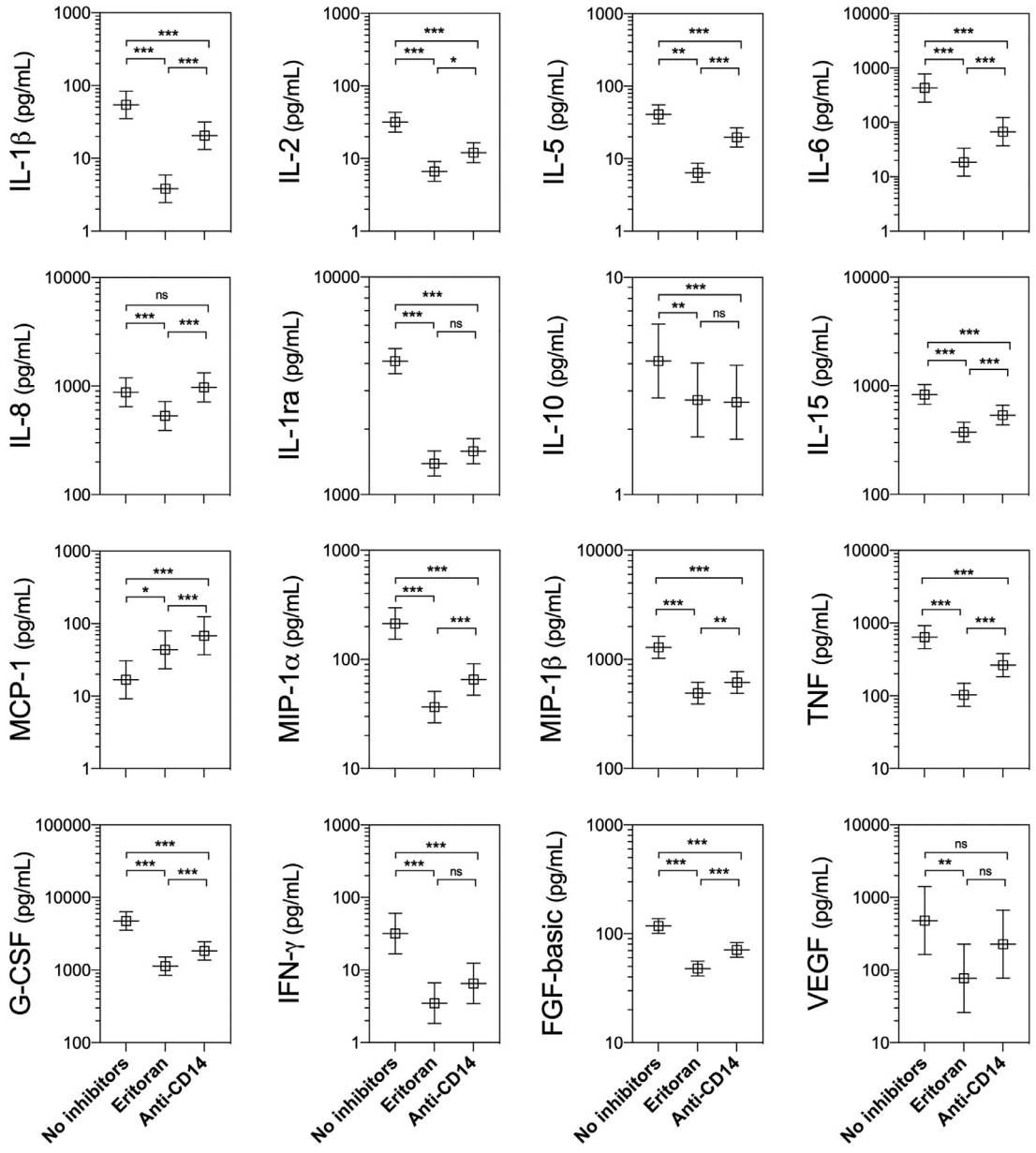

Fig. 6. Comparison of Eritoran and CD14 inhibition on cytokine release induced by the decellularized porcine cornea (DPC) in human whole blood. Effects of both inhibitors were measured in five individual human donor blood samples, where cytokine-release was induced by DPC (total of ten porcine cornea pieces). Data are presented as margin plots. Horizontal lines in boxes represent the mean of DPC induced cytokines with no inhibitors, Eritoran, or anti-CD14. The error bars show the 95% confidence intervals. Statistical significance was estimated by using mixed-effect models of log-transformed data that compared the control condition with each other condition and planned Wald tests of other paired comparisons. Significance levels are denoted as star (*) where, * $p \leq 0.05$, ** $p \leq 0.017$, and *** $p \leq 0.001$.

1ra, IL-10, IL-15, MCP-1, MIP-1α, MIP-1β, TNF, IFN-γ and FGF-basic), whereas, anti-CD14 inhibited ($p \leq 0.017$) twelve (IL-1β, IL-2, IL-5, IL-6, IL-1ra, IL-10, IL-15, MIP-1α, MIP-1β, TNF, IFN-γ and FGF-basic). The combined blockade of C5 and CD14 reduced ($p \leq 0.017$) expression of all of the cytokines that otherwise were increased by exposure to corneas. Although both blockade of C5 and CD14 can interchangeably inhibit a range of cytokines induced by NPC when used alone, IL-8, and MCP-1 differed from the others by being highly complement-dependent (Fig. 5). Combined blocked showed a synergistic inhibitory effect which reduced of IL-6, IL-8, MIP-1α, MIP-1β, IFN-γ, and G-CSF even more efficiently ($p \leq 0.017$) compared to the single-inhibition either by anti-C5 or anti-CD14 alone.

None of the DPC- and g-DPC induced cytokines were inhibited ($p>0.017$) by anti-C5 alone. For DPC, anti-CD14 alone significantly inhibited thirteen cytokines (IL-1β, IL-2, IL-5, IL-6, IL-8, IL-1ra, IL-10, IL-15, MIP-1β, TNF, IFN-γ, FGF-basic, and VEGF).

The combined blockade of C5 and CD14 showed a synergistic effect by inhibiting an additional cytokine, MCP-1, along with the cytokines mentioned above. In the case of g-DPC induced cytokines, anti-CD14 alone significantly inhibited fourteen cytokines (IL-1β, IL-2, IL-5, IL-6, IL-8, IL-1ra, IL-15, MIP-1α, MIP-1β, TNF, G-CSF, IFN-γ, FGF-basic, and VEGF), whereas, the combined blockade of C5 and CD14 inhibited an additional cytokine, MCP-1. Moreover, combined blockade showed synergistic effect ($p \leq 0.0001$) in reducing IL-8 and IFN-γ compared to the single inhibition either by anti-C5 or anti-CD14 alone.

Finally, we investigated whether TLR4 could be responsible for the substantial inhibitory effect of CD14, since CD14 is the main co-receptor for TLR4, in addition to TLR2 and others. The LPS

analogue, Eritoran binds competitively to the TLR4-MD2 complex, and thus is highly specific for TLR4. Treatment with Eritoran was compared with the inhibition of CD14 (Fig. 6). Importantly, Eritoran inhibited ($p > 0.017$) the same fourteen cytokines (IL-1β, IL-2, IL-5, IL-6, IL-8, IL-1ra, IL-15, MIP-1α, MIP-1β, TNF, G-CSF, IFN-γ, FGF-basic, and VEGF) that were inhibited by anti-CD14 either to a greater degree (IL-1β, IL-5, IL-6, IL-8, IL-15, MIP-1α, MIP-1β, TNF, G-CSF and FGF-basic) or to the same extent (IL-2, IL-1ra, and IFN-γ). Unlike anti-CD14, Eritoran inhibited IL-8 and VEGF as well (Fig. 6).

4. Discussion

Among the corneal treatments evaluated here, *i.e.,* NPC, DPC, g-DPC, only NPC activated the complement system, but all of them induced the release of cytokines in various degrees. To the best of our knowledge, this is the first demonstration that the cornea induced inflammatory responses profoundly dependent on both C5 and CD14 receptor activation, which can be reduced by using therapeutic inhibition. Moreover, combined blockade of C5 with CD14 in human whole blood demonstrated a synergistic effect in inhibiting important cytokines, such as IL-6, IL-8, MIP-1α, MIP-1β, MCP-1, G-CSF, and IFN-γ depending on the form of xenograft.

For NPC-induced response, anti-C5 alone could significantly inhibit more cytokines than by anti-CD14 alone. The combined blockade, however, inhibited all sixteen cytokines. This result infers that the complement C5 plays a greater role than CD14 for the release of cytokines induced by NPC. This explanation is corroborated by the observation of complement activation by NPC measured both by deposition on the corneal surface and the fluid phase markers in the plasma. A substantial redundancy of all these systems is a reasonable explanation for such findings [40,41].

The NPC, when in contact with human whole blood, activated the complement system (Fig. 3 A). Unlike DPC and g-DPC, the NPC has corneal cells. However, these cells in NPC cannot produce any complement proteins or cytokines because all xenografts were glycerol-preserved until their use in the experiments. After the incubation, the cornea was removed from the whole blood before preparing the plasma sample for the detection of complement activation and cytokine level. Therefore, the results are not interfered by the local production of complement proteins or cytokines by the corneal cells. Modification of porcine cornea by decellularization significantly reduced complement activation, which was shown in this study by both the absence of complement deposition on DPC and fluid-phase activation (Fig. 3 A and B). Nevertheless, DPC elevated the cytokines at the highest magnitude between the three forms of the cornea. Unlike NPC, the cytokine-release induced by the DPC was exclusively mediated by CD14, which, by blocking, significantly inhibited twelve cytokines. None of the cytokines released were inhibited by anti-C5 alone. However, MCP-1 inhibition could only be achieved by a combined blockade of C5 and CD14. The lack of an effect of anti-C5 on cytokine expression is plausibly due to the absence of cellular components in the decellularized cornea, which appeared to be responsible for complement-mediated cytokine-release. The release of a higher level of cytokines and their inhibition by anti-CD14 alone can be attributed to the change of xenograft's functional property from complement-inducing to TLR-inducing. This change might be due to exposure of new ligands in the corneal stroma exposed by decellularization [42].

In g-DPC, many overlapping cytokines were inhibited both by anti-CD14 alone and the combination of anti-C5 and anti-CD14 as compared to their effect in inhibiting cytokines induced by DPC. Gamma irradiation is a recommended method to sterilize DPC, given that the irradiation does not adversely alter corneal mechanical properties [15]. We used a previously reported protocol to render NPC into DPC and g-DPC, confirming in this study its efficiency by examining random samples through transmission electron microscopy and histological staining. We reproduced the previously reported results but added new findings. For instance, we found that gamma-irradiation of DPC may lower the release of cytokines and may thereby improve biocompatibility. IL-1β, and IL-10 expression in whole blood were significantly reduced by gamma-irradiation of the cornea, although still significantly higher than background levels. None of the cytokines were inhibited by anti-C5 alone. Here again, the blockade of C5, together with CD14, demonstrated a synergistic effect by inhibiting IL-8, MCP-1, and IFN-γ.

Several independent studies have established the association between complement activation and corneal xenograft rejection, evaluated either in the systemic circulation, aqueous humor, and/or deposition on the xenograft surface in pig-to-rhesus macaque [14,21] and pig-to-mouse [20]. The blockade of complement activation and CD14 to reduce early inflammatory response is a method which has been tested in a series of studies in various disease models using whole blood as well as mice and pig models with promising results [32,40,43–45]. To our knowledge, ours is the first report identifying a role for CD14, mediated through TLR4, in the corneal xenograft-induced inflammatory response in human blood.

Irrespective of the three forms of corneal tissue used here, a combined blockade of C5 and CD14 reduced the level of most cytokines. The findings are clinically relevant as there is increasing evidence of a systemic inflammatory response to the presence of a porcine xenograft in recipients. However, in the case of corneal transplantation, the intensity of the systemic inflammation is not well documented in human studies. In one recent clinical study, rejection of porcine g-DPC in a human patient was associated with significant increases of IL-2 and INF-γ [13]. Both cytokines were found to be elevated in the current study as well (Fig. 4). Anti-CD14 alone, or together with anti-C5, significantly inhibited IL-2 and INF-γ (Fig. 5). In the porcine g-DPC placed in a human patient, other cytokines such as IL-1, IL-8, and TNF remained undetected. In contrast, we observed elevations of both in whole blood. All were inhibited significantly either by anti-CD14 alone or together with anti-C5. In the case of MCP-1, combined blockade showed evidence of synergistic inhibition. Looking at the overall trend of cytokine-release and their inhibition, we can reasonably generalize that the porcine xenograft-induced release of IL-1β, L-2, IL-6, IL-8, MCP-1, MIP-1β, TNF and IFN-γ are both complement and TLR4 mediated [32,46,47].

A possible limitation of our study is that we tested the innate immune responses to corneal xenografts in human blood, while the cornea is an avascular tissue as well as an immune-privileged site. However, the evaluation of innate immune response in *ex vivo* human whole blood by corneal xenograft is relevant as for other biomaterials. The relevance of using blood for this purpose lies in the practicality of corneal xenotransplantation. The recipient eyes that would be indicated for corneal xenograft typically suffer from severe pathologic conditions, and would have lost immune privilege and be highly vascularized [48,49]. Moreover, upon transplantation, the cornea encounters other body fluids, *i.e.*, tear film and aqueous humor, that may contain immunologic components such as complement proteins and soluble TLRs. This study also did not take into account possible contributions of tissue-resident macrophages and antigen-presenting cells of the host cornea and their implication in the modulation of tissue inflammation. Since the *in vivo* system is more complex, our finding is not directly translatable to the clinical situation, but it provides important mechanistic insight of innate immunity in graft rejection.

Nevertheless, the complement system is crucial in hyperacute organ rejection. A study showed that pig kidneys perfused with human whole blood *ex vivo* survived longer if the complement sys-

tem was blocked at the C3 level [50]. C5 inhibitors (eculizumab and zilucoplan) are in regular clinical use for the treatment of four rare diseases (paroxysmal nocturnal hemoglobinuria, atypical hemolytic syndrome, myasthenia gravis and neuromyelitis optica spectrum diseases). Therapeutic C5-inhibition is well established, eculizumab has been in clinical use for more than ten years [51]. CD14 inhibition is not used in the clinic, but promising results had been demonstrated in experimental models, including baboon sepsis treated with an antibody blocking CD14 [52]. We regard that our human blood model provides important mechanistic insight into rejection mechanisms, relevant for corneal xenografts for human implantation.

5. Conclusion

We conclude that combined blockade of C5 and CD14 synergistically inhibited porcine cornea induced innate inflammatory responses. Based on the comparison of CD14 and TLR4 inhibition, we postulate that a combination of C5 and TLR4 inhibition is a potential therapeutic approach in pig-to-human corneal xenotransplantation.

Data availability

The data that support the findings of this study are available from the corresponding author, RI, upon reasonable request.

Declaration of Competing Interest

The authors declare that they have no known competing financial interests or personal relationships that could have appeared to influence the work reported in this paper.

Acknowledgement

This work was supported by Helse Sør-Øst RHF (project number 2016101), Norway along with Boston-KPro research fund, Boston, MA, USA and Andalusian Regional Ministry of Health grant (project number PIGE-0194-2019), Spain.

References

[1] I. Brunette, C.J. Roberts, F. Vidal, M. Harissi-Dagher, J. Lachaine, H. Sheardown, G.M. Durr, S. Proulx, M. Griffith, Alternatives to eye bank native tissue for corneal stromal replacement, Prog. Retin. Eye Res. 59 (2017) 97–130.
[2] P. Gain, R. Jullienne, Z. He, M. Aldossary, S. Acquart, F. Cognasse, G. Thuret, Global survey of corneal transplantation and eye banking, JAMA Ophthalmol. 134 (2) (2016) 167–173.
[3] R. Kissam, Ceratoplastice in man, N.Y. J. Med. Collat. Sci. 2 (1844) 281–282.
[4] Artificial cornea, Lancet 138 (3555) (1891) 886.
[5] T.H.K.K.M. Durrani, M.M. Hassan, S.M. Rizvi, J.C. Tanner, J.J. Vandeput, Penetrating keratoplasty with purified bovine collagen: report of a coordinated trial on fifteen human cases, Ann. Ophthalmol. 6 (1974) 639–646.
[6] M. Haq, Fish cornea for grafting, Br. Med. J. 2 (5815) (1972) 712–713.
[7] N.R.B. Soomsawasdi, S. Bhadrakom, Hetero-keratoplasy using gibbon donor corneae, Asia Pacific Acad. Ophthalmol. 2 (1964) 251–261.
[8] G. De Ocampo, R. Sunga, C. De La Cruz-Estrella, The use of chicken and monkey cornea for human corneal grafting, Acta Med. Philipp. 16 (1959) 55–64.
[9] H.J. Choi, C.H. Yoon, J.Y. Hyon, H.K. Lee, J.S. Song, T.Y. Chung, H. Mo, J. Kim, J.E. Kim, B.J. Hahm, J. Yang, W.B. Park, M.K. Kim, Protocol for the first clinical trial to investigate safety and efficacy of corneal xenotransplantation in patients with corneal opacity, corneal perforation, or impending corneal perforation, Xenotransplantation 26 (1) (2019) e12446.
[10] V. Lamm, H. Hara, A. Mammen, D. Dhaliwal, D.K. Cooper, Corneal blindness and xenotransplantation, Xenotransplantation 21 (2) (2014) 99–114.
[11] H. Hara, D.K. Cooper, Xenotransplantation–the future of corneal transplantation? Cornea 30 (4) (2011) 371–378.
[12] M.K. Kim, H. Hara, Current status of corneal xenotransplantation, Int. J. Surg. (London, England) 23 (Pt B) (2015) 255–260.
[13] Y. Shi, T. Bikkuzin, Z. Song, X. Jin, H. Jin, X. Li, H. Zhang, Comprehensive evaluation of decellularized porcine corneal after clinical transplantation, Xenotransplantation 24 (6) (2017), doi:10.1111/xen.12338.
[14] H.J. Choi, M.K. Kim, H.J. Lee, J.H. Ko, S.H. Jeong, J.I. Lee, B.C. Oh, H.J. Kang, W.R. Wee, Efficacy of pig-to-rhesus lamellar corneal xenotransplantation, Invest. Ophthalmol. Vis. Sci. 52 (9) (2011) 6643–6650.
[15] M.M. Islam, R. Sharifi, S. Mamodaly, R. Islam, D. Nahra, D.B. Abusamra, P.C. Hui, Y. Adibnia, M. Goulamaly, E.I. Paschalis, A. Cruzat, J. Kong, P.H. Nilsson, P. Argueso, T.E. Mollnes, J. Chodosh, C.H. Dohlman, M. Gonzalez-Andrades, Effects of gamma radiation sterilization on the structural and biological properties of decellularized corneal xenografts, Acta Biomater. 96 (2019) 330–344.
[16] A. Isidan, S. Liu, P. Li, M. Lashmet, L.J. Smith, H. Hara, D.K.C. Cooper, B. Ekser, Decellularization methods for developing porcine corneal xenografts and future perspectives, Xenotransplantation (2019) e12564-e12564.
[17] S.F. Badylak, Xenogeneic extracellular matrix as a scaffold for tissue reconstruction, Transpl. Immunol. 12 (3–4) (2004) 367–377.
[18] S.W. Wee, S.U. Choi, J.C. Kim, Deep anterior lamellar keratoplasty using irradiated acellular cornea with amniotic membrane transplantation for intractable ocular surface diseases, Korean J. Ophthalmol. 29 (2) (2015) 79–85.
[19] W. Stevenson, S.-F. Cheng, P. Emami-Naeini, J. Hua, E.I. Paschalis, R. Dana, D.R. Saban, Gamma-irradiation reduces the allogenicity of donor corneas, Invest. Ophthalmol. Vis. Sci. 53 (11) (2012) 7151–7158.
[20] J.Y. Oh, M.K. Kim, H.J. Lee, J.H. Ko, Y. Kim, C.S. Park, H.J. Kang, C.G. Park, S.J. Kim, J.H. Lee, W.R. Wee, Complement depletion with cobra venom factor delays acute cell-mediated rejection in pig-to-mouse corneal xenotransplantation, Xenotransplantation 17 (2) (2010) 140–146.
[21] J. Kim, D.H. Kim, H.J. Choi, H.J. Lee, H.J. Kang, C.-G. Park, E.-S. Hwang, M.K. Kim, W.R. Wee, Anti-CD40 antibody-mediated costimulation blockade promotes long-term survival of deep-lamellar porcine corneal grafts in non-human primates, Xenotransplantation 24 (3) (2017), doi:10.1111/xen.12298.
[22] T. Schick, M. Steinhauer, A. Aslanidis, L. Altay, M. Karlstetter, T. Langmann, M. Kirschfink, S. Fauser, Local complement activation in aqueous humor in patients with age-related macular degeneration, Eye (2017).
[23] N.S. Bora, C.L. Gobleman, J.P. Atkinson, J.S. Pepose, H.J. Kaplan, Differential expression of the complement regulatory proteins in the human eye, Invest. Ophthalmol. Vis. Sci. 34 (13) (1993) 3579–3584.
[24] A. Esposito, B. Suedekum, J. Liu, F. An, J. Lass, M.G. Strainic, F. Lin, P. Heeger, M.E. Medof, Decay accelerating factor is essential for successful corneal engraftment, Am. J. Transpl.: Off. J. Am. Soc. Transpl. Am. Soc. Transplant Surg. 10 (3) (2010) 527–534.
[25] T. Li, W. Lee, H. Hara, C. Long, M. Ezzelarab, D. Ayares, H. Huang, Y. Wang, C.T. Esmon, D.K.C. Cooper, H. Iwase, An investigation of extracellular histones in pig-to-baboon organ xenotransplantation, Transplantation 101 (10) (2017) 2330–2339.
[26] C.T. Esmon, Molecular circuits in thrombosis and inflammation, Thromb. Haemost. 109 (3) (2013) 416–420.
[27] R. Sharifi, Y. Yang, Y. Adibnia, C.H. Dohlman, J. Chodosh, M. Gonzalez-Andrades, Finding an optimal corneal xenograft using comparative analysis of corneal matrix proteins across species, Sci. Rep. 9 (1) (2019) 1876.
[28] P. Seifert, Modified Hiraoka TEM grid staining apparatus and technique using 3D printed materials and gadolinium triacetate tetrahydrate, a nonradioactive uranyl acetate substitute, J. Histotechnol. 40 (4) (2017) 130–135.
[29] T.E. Mollnes, O.L. Brekke, M. Fung, H. Fure, D. Christiansen, G. Bergseth, V. Videm, K.T. Lappegard, J. Kohl, J.D. Lambris, Essential role of the C5a receptor in E coli-induced oxidative burst and phagocytosis revealed by a novel lepirudin-based human whole blood model of inflammation, Blood 100 (5) (2002) 1869–1877.
[30] C. Lau, K.S. Gunnarsen, L.S. Høydahl, J.T. Andersen, G. Berntzen, A. Pharo, J.K. Lindstad, J.K. Ludviksen, O.-L. Brekke, A. Barratt-Due, E.W. Nielsen, C.R. Stokes, T. Espevik, I. Sandlie, T.E. Mollnes, Chimeric anti-CD14 IGG2/4 Hybrid antibodies for therapeutic intervention in pig and human models of inflammation, J. Immunol. (Baltimore, Md.: 1950) 191 (9) (2013) 4769–4777.
[31] C. Lau, M.B. McAdam, G. Bergseth, A. Grevys, J.A. Bruun, J.K. Ludviksen, H. Fure, T. Espevik, A. Moen, J.T. Andersen, T.E. Mollnes, NHDL, a recombinant V(L)/V(H) hybrid antibody control for IgG2/4 antibodies, MAbs 12 (1) (2020) 1686319-1686319.
[32] A.M. Thomas, A. Gerogianni, M.B. McAdam, Y. Fløisand, C. Lau, T. Espevik, P.H. Nilsson, T.E. Mollnes, A. Barratt-Due, Complement component C5 and TLR molecule CD14 mediate heme-induced thromboinflammation in human blood, J. Immunol. (Baltimore, Md.: 1950) 203 (6) (2019) 1571–1578.
[33] B.R. Oppedal, P.J. Bohler, P.F. Marton, P. Brandtzaeg, Carcinoma of the nasopharynx. Histopathological examination with supplementary immunohistochemistry, Histopathology 11 (11) (1987) 1161–1169.
[34] G. Bergseth, J.K. Ludviksen, M. Kirschfink, P.C. Giclas, B. Nilsson, T.E. Mollnes, An international serum standard for application in assays to detect human complement activation products, Mol. Immunol. 56 (3) (2013) 232–239.
[35] G.J. Wolbink, J. Bollen, J.W. Baars, R.J. ten Berge, A.J. Swaak, J. Paardekooper, C.E. Hack, Application of a monoclonal antibody against a neoepitope on activated C4 in an ELISA for the quantification of complement activation via the classical pathway, J. Immunol. Methods 163 (1) (1993) 67–76.
[36] P. Garred, T.E. Mollnes, T. Lea, E. Fischer, Characterization of a monoclonal antibody MoAb bH6 reacting with a neoepitope of human C3 expressed on C3b, iC3b, and C3c, Scand. J. Immunol. 27 (3) (1988) 319–327.
[37] T.E. Mollnes, T. Lea, M. Harboe, J. Tschopp, Monoclonal antibodies recognizing a neoantigen of poly(C9) detect the human terminal complement complex in tissue and plasma, Scand. J. Immunol. 22 (2) (1985) 183–195.

[38] T.E. Mollnes, H. Redl, K. Høgåsen, A. Bengtsson, P. Garred, L. Speilberg, T. Lea, M. Oppermann, O. Götze, G. Schlag, Complement activation in septic baboons detected by neoepitope-specific assays for C3b/iC3b/C3c, C5a and the terminal C5b-9 complement complex (TCC), Clin. Exp. Immunol. 91 (2) (1993) 295–300.
[39] A.J. Sankoh, M.F. Huque, S.D. Dubey, Some comments on frequently used multiple endpoint adjustment methods in clinical trials, Stat. Med. 16 (22) (1997) 2529–2542.
[40] A. Barratt-Due, S.E. Pischke, P.H. Nilsson, T. Espevik, T.E. Mollnes, Dual inhibition of complement and toll-like receptors as a novel approach to treat inflammatory diseases-C3 or C5 emerge together with CD14 as promising targets, J. Leukoc. Biol. (2016).
[41] A. Barratt-Due, S.E. Pischke, O.L. Brekke, E.B. Thorgersen, E.W. Nielsen, T. Espevik, M. Huber-Lang, T.E. Mollnes, Bride and groom in systemic inflammation–the bells ring for complement and toll in cooperation, Immunobiology 217 (11) (2012) 1047–1056.
[42] G.W. Kiyeko, E. Hatterer, S. Herren, I. Di Ceglie, P.L. van Lent, W. Reith, M. Kosco-Vilbois, W. Ferlin, L. Shang, Spatiotemporal expression of endogenous TLR4 ligands leads to inflammation and bone erosion in mouse collagen-induced arthritis, Eur. J. Immunol. 46 (11) (2016) 2629–2638.
[43] O.L. Brekke, D. Christiansen, H. Fure, A. Pharo, M. Fung, J. Riesenfeld, T.E. Mollnes, Combined inhibition of complement and CD14 abolish E. coli-induced cytokine-, chemokine- and growth factor-synthesis in human whole blood, Mol. Immunol. 45 (14) (2008) 3804–3813.
[44] A.M. Thomas, C. Schjalm, P.H. Nilsson, P.H.H. Lindenskov, R. Rortveit, R. Solberg, O.D. Saugstad, M.M. Berglund, P. Stromberg, C. Lau, T. Espevik, J.H. Jansen, A. Castellheim, T.E. Mollnes, A. Barratt-Due, Combined inhibition of C5 and CD14 attenuates systemic inflammation in a piglet model of meconium aspiration syndrome, Neonatology 113 (4) (2018) 322–330.
[45] B.C. Hellerud, H.L. Orrem, K. Dybwik, S.E. Pischke, A. Baratt-Due, A. Castellheim, H. Fure, G. Bergseth, D. Christiansen, M.A. Nunn, T. Espevik, C. Lau, P. Brandtzaeg, E.W. Nielsen, T.E. Mollnes, Combined inhibition of C5 and CD14 efficiently attenuated the inflammatory response in a porcine model of meningococcal sepsis, J. Intensive Care 5 (2017) 21.
[46] N. Niyonzima, B. Halvorsen, B. Sporsheim, P. Garred, P. Aukrust, T.E. Mollnes, T. Espevik, Complement activation by cholesterol crystals triggers a subsequent cytokine response, Mol. Immunol. 84 (2017) 43–50.
[47] P. Orning, K.S. Hoem, A.E. Coron, G. Skjak-Braek, T.E. Mollnes, O.L. Brekke, T. Espevik, A.M. Rokstad, Alginate microsphere compositions dictate different mechanisms of complement activation with consequences for cytokine release and leukocyte activation, J. Controll. Release : Off. J. Controll. Release Soc. 229 (2016) 58–69.
[48] J.Y. Niederkorn, Corneal transplantation and immune privilege, Int. Rev. Immunol. 32 (1) (2013) 57–67.
[49] J.V. Forrester, H. Xu, Good news-bad news: the Yin and Yang of immune privilege in the eye, Front. Immunol. 3 (2012) 338.
[50] A.E. Fiane, T.E. Mollnes, V. Videm, T. Hovig, K. Hogasen, O.J. Mellbye, L. Spruce, W.T. Moore, A. Sahu, J.D. Lambris, Compstatin, a peptide inhibitor of C3, prolongs survival of ex vivo perfused pig xenografts, Xenotransplantation 6 (1) (1999) 52–65.
[51] D. Ricklin, A. Barratt-Due, T.E. Mollnes, Complement in clinical medicine: clinical trials, case reports and therapy monitoring, Mol. Immunol. 89 (2017) 10–21.
[52] R.S. Keshari, R. Silasi, N.I. Popescu, G. Regmi, H. Chaaban, J.D. Lambris, C. Lupu, T.E. Mollnes, F. Lupu, CD14 inhibition improves survival and attenuates thrombo-inflammation and cardiopulmonary dysfunction in a baboon model of Escherichia coli sepsis, J. Thromb. Haemost. (2020).